THE JOURNAL OF PHYSICAL CHEMISTRY B

Article

pubs.acs.org/JPCB

Nanouidic Compaction of DNA by Like-Charged Protein

Ce Zhang,[†] Zongying Gong,[†] Durgarao Guttula,[†] Piravi P. Malar,[†] Jeroen A. van Kan,[†] Patrick S. Doyle,[‡,§] and Johan R. C. van der Maarel*[,†,§]

[†]Department of Physics, National University of Singapore, Singapore 117542

[‡]Department of Chemical Engineering, Massachusetts Institute of Technology, Cambridge, Massachusetts 02139, United States

[§]BioSystems and Micromechanics (BioSyM) IRG, Singapore−MIT Alliance for Research and Technology (SMART) Centre, Singapore

ABSTRACT: The effects of the like-charged proteins bovine serum albumin and hemoglobin on the conformation and compaction of single DNA molecules confined in rectangular nanochannels were investigated with fluorescence microscopy. The channels have lengths of 50 μm and cross-sectional diameters in the range of 80−300 nm. In the wider channels, the DNA molecules are compressed and eventually condense into a compact form with increasing concentration of protein. In the narrow channels, no condensation was observed. The threshold concentration for condensation depends on the channel cross-sectional diameter as well as the ionic strength of the supporting medium. The critical values for full compaction are typically less than one-tenth of a millimolar. In the bulk phase and in the same environmental conditions, no condensation was observed. Anisotropic nanoconfinement hence facilitates compaction of DNA by negatively charged protein. We tentatively interpret this behavior in terms of enhanced depletion interaction between segments of the DNA molecule due to orientation order imposed by the channel walls.

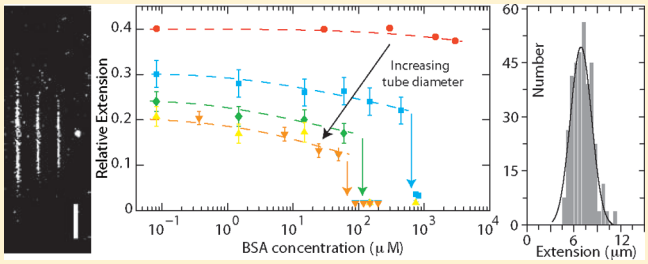

I. INTRODUCTION

A substantial amount of biomacromolecules do not directly participate in biochemical reactions. Nevertheless, these background species have an effect on molecular transport, reaction rates, and chemical equilibrium.[1] They also affect macromolecular conformation. An example is the transition of DNA to a compact form (condensation) in the presence of simple salts and overthreshold concentrations of neutral polymers.[2−4] It has been proposed that crowding is the basis for phase separation in the cytoplasm.[5,6] The latter hypothesis is supported by the observation that DNA can be condensed by cytoplasmic extracts from *Escherichia coli* at extract concentrations corresponding to about 1/2 the cellular concentration.[7] Besides background species, the cytoplasm of most eukaryotic cells contains stationary elements such as fiber lattices and membranes. These structures affect macromolecular conformation through confinement in one or two-dimensions. Accordingly, crowding and confinement are intimately related and deserve an integrated approach in order to understand their modes of operation and how they couple.

DNA condensation can be assisted and directed by a surface. In surface-directed condensation, DNA is first adsorbed onto an interface, after which it is condensed with an agent. Examples are the condensation of single molecules into rods and toroidal structures with protamine or ethanol.[8,9] Single DNA molecules can be confined and visualized with fluorescence microscopy in quasi two-dimensional nanoslits or one-dimensional nanochannels. The extension in the longitudinal direction of nanochannels has been measured as a function of channel diameter[10,11] and ionic strength of the supporting medium.[12,13] We have reported the effect of the generic crowding agent dextran on the conformation and condensation of DNA confined in long, straight, and rectangular nanochannels with a depth of 300 nm and a width in the range of 150−300 nm.[14] It was observed that the confined DNA molecules initially elongate and eventually condense into a compact form with increasing concentration of dextran. The critical concentration for condensation depends on the dextran molecular weight. In contrast to the situation in the bulk phase, crowding-induced condensation of DNA in a nanochannel does not require a high concentration of salt.[2−4] In nanoslit confinement, the DNA molecule also initially swells, but does not show an abrupt transition to a compact globular form.[15] Reduction in coil size in nanoslits occurs over a large range of dextran concentration and does not compact to the same extent as in tubes. These results show that confinement geometry plays a pivotal role in DNA response to crowding.

In the bulk phase and at high concentrations of salt (>100 mM NaCl), Yoshikawa et al. have shown that DNA can be compacted into a globular form by like-charged protein bovine serum albumin (BSA, 66.4 kDa, p *I* 4.9).[16] Here, we report the effect of BSA as well as hemoglobin (Hb, 68.0 kDa, p *I* 7.1) on the conformation and compaction of single DNA molecules confined in quasi one-dimensional nanochannels with average

Received: December 27, 2011
Revised: February 8, 2012
Published: February 9, 2012

cross-sectional diameters in the range of 80−300 nm. BSA and Hb have molecular dimensions of 14 × 3.8 × 3.8 and 6.4 × 5.5 × 5.0 nm^3, respectively. Furthermore, they are both negatively charged at the relevant pH of 8.5. The effective charge of BSA is −15 and, based on the ζ potential, the effective charge of Hb is around −5.[17,18] We also report supplementary results obtained with neutral dextran nanoparticles with a radius of gyration of R_g = 6.9 nm (M_w = 50 kDa).

Our experiments were done using devices made of poly(dimethyl siloxane) (PDMS). We use a lithography process with proton beam writing to make a nanopatterned stamp.[19,20] The stamp is subsequently replicated in PDMS, followed by curing and sealing with a glass slide.[21] Around 100 chips can be replicated using a single stamp, so that we have used a fresh chip for every experiment. A series of channels was produced with a depth down to 60 nm and minimum width of 100 nm. T4-DNA (166 kbp) and λ-DNA (48.5 kbp) molecules were visualized with fluorescence microscopy. In most experiments, T4-DNA was stained with YOYO-1 with an intercalation ratio of 23 base-pairs per dye molecule. For such a low level of intercalation, the distortion of the secondary DNA structure is minimal; the contour length increases from 57 to 60 μm, and the DNA charge is reduced by a factor of 42/46.[22,23] Furthermore, there is no appreciable effect on the bending rigidity, as inferred from previously reported measurements of the extension of DNA in nanochannels with different concentrations of dye.[13] λ-DNA was stained with Alexa Fluor 546.[24] Alexa dye is anionic and covalently attached to the DNA molecule. DNA molecules were brought into the channels with an electric field or pressure, and their extensions were measured in buffers of various ionic strength and various concentrations of BSA, Hb, or dextran. We have also monitored the condensation of DNA for overthreshold protein concentrations. For reference, the effect of protein on the size of T4-DNA in the bulk phase was measured with fluorescence microscopy.

II. EXPERIMENTAL PROCEDURES

A. Fabrication of the Nanofluidic Chips. The nanofluidic devices were made by replication in PDMS of patterned master stamps.[13] The stamps were fabricated in HSQ resist (Dow Corning, Midland, MI) using a lithography processes with proton beam writing.[19,20] The 60 ± 5, 200 ± 5, 250 ± 5, and 300 ± 5 nm heights of the positive channel structures on the stamps were measured with atomic force microscopy (Dimension 3000, Veeco, Woodbury, NY). The stamps were replicated in PDMS followed by curing with a curing agent (Sylgard, Dow Corning) at 337 K for 24 h.[21] Finally, the PDMS replicas were sealed with glass slides after both substrates were plasma oxidized (Harrick, Ossining, NY). The widths of the channels in the PDMS replicas were measured with atomic force microscopy, and the values agreed with those obtained from the scanning electron microscopy images of the HSQ master stamps. The nanochannels have a length of 50 μm and rectangular cross sections of 100 × 60, 300 × 200, 100 × 250, 200 × 250, 300 × 250, and 300 × 300 nm^2.

B. Sample Preparation. T4-DNA was purchased from Nippon Gene, Tokyo and used without further purification. λ-DNA was purchased from New England Biolabs, Ipswich, MA. YOYO-1 and Alexa Fluor 546 were purchased from Invitrogen, Carlsbad, CA. λ-DNA was covalently stained with Alexa Fluor 546.[24] T4-DNA was stained with YOYO-1 with an intercalation ratio of 23 or 100 base-pairs per dye molecule. Samples were prepared by dialyzing solutions of DNA against 10 mM Tris/HCl or 10 mM Tris/HCl with 25 mM NaCl in microdialyzers. The Tris/HCl concentration is 10 mM Tris adjusted with HCl to pH 8.5, i.e., 2.9 mM TrisCl and 7.1 mM Tris. BSA, Hb, and dextran were purchased from Sigma-Aldrich and dissolved in the relevant buffer. Solutions of protein or dextran and DNA were subsequently mixed in equal volumes and incubated for 24 h at 277 K. The final DNA concentration is 0.003 g/L. No anti-photobleaching agent was used. The ionic strength of the buffer was calculated with the Davies equation for estimating the activity coefficients of the ions and a dissociation constant pK = 8.08 for Tris.

C. Fluorescence Imaging. The stained DNA molecules dispersed in the relevant solution were loaded into one of the two reservoirs connected by the nanochannels. In most experiments, the DNA molecules were subsequently driven into the channels by electrophoresis. For this purpose, two platinum electrodes were immersed in the reservoirs and connected to an electrophoresis power supply with a relatively low voltage in the range of 0.1−10 V (Keithley, Cleveland, Ohio). Once the DNA molecules were localized inside the nanochannels, the electric field was switched off, and the molecules were allowed to relax to their equilibrium state for at least 60 s. In some experiments, the molecules were driven into the channels using a microinjector with a minimal injection pressure of 0.7 kPa (Narishige, Tokyo). The stained DNA molecules were visualized with a Nikon Eclipse Ti inverted fluorescence microscope equipped with a 200 W metal halide lamp, a filter set, and a 100× oil immersion objective. The exposure time was controlled by a UV light shutter. Images were collected with an electron multiplying charge coupled device (EMCCD) camera (Andor iXon X3), and the extension of the DNA molecules inside the channels was measured with ImageJ software (http://rsb.info.nih.gov/ij/).

D. Bulk Phase Imaging. A droplet of solution was deposited on a microscopy slide and sealed with a coverslip separated by a 0.12 mm spacer. The YOYO-1 stained T4-DNA molecules were imaged with a Nikon Eclipse Ti microscope and a 100× oil immersion objective. Video was collected with an EMCCD camera (Andor iXon X3). For each sample, around 10 min of video was analyzed with Matlab (Natick, MA) and the sizes of the molecules were obtained with public domain tracking software (http://physics.georgetown.edu/matlab/).

III. RESULTS

Montages of images of single T4-DNA molecules confined in rectangular nanochannels with a cross-section of 200 × 300 nm^2 are shown in Figure 1. The images refer to well-equilibrated conformations. After the electric field has been switched off, the molecules relax to their equilibrium state within 60 s. We have verified that there is no further change in the extension of the molecules for more than 3 h. Furthermore, we observed no difference in extension between molecules inserted by electrophoresis or pressure. Video imaging was started 5−10 min after the molecules were brought into the channels and lasted for another 10 min. The equilibrated molecules are slightly contracted in the longitudinal direction of the channel with respect to the protein-free state. For overthreshold concentrations of protein and wider channels, condensation of the DNA molecules into a compact form is observed. In the case of the relatively narrow 60 × 100 nm^2 channel, the molecules remain elongated irrespective of protein concentration. Condensed DNA is visible as a bright

dx.doi.org/10.1021/jp2124907 | J. Phys. Chem. B 2012, 116, 3031−3036

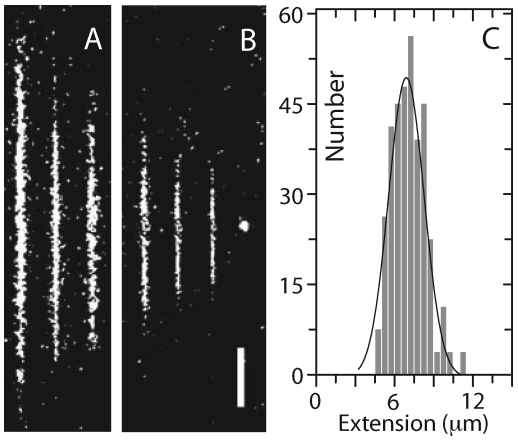

Figure 1. (A) Montage of fluorescence images of T4-DNA in 200 × 300 nm^2 channels in 10 mM Tris/HCl (pH 8.5). From left to right, the molecule is protein-free, in 7.4 μM Hb, and in 7.4 μM BSA. (B) As in panel A, but in 10 mM Tris/HCl with 25 mM NaCl. From left to right: protein-free, 7.4 μM Hb, 4.4 μM BSA, and 17.7 μM BSA (condensed). The scale bar denotes 2 μm. (C) Distribution in extension of a population of 330 molecules in 10 mM Tris/HCl with 25 mM NaCl. A Gaussian fit gives a mean extension of $R_{\|} = 7 \pm 2$ μm.

fluorescence spot and can easily be discerned from the extended form.

We have measured the extension of the DNA molecules confined in the nanochannels. For each experimental condition, we have used a fresh PDMS replica and measured around 200 molecules. The fluctuation-induced distribution in extension is close to Gaussian.[25] An example of such a distribution is also shown in Figure 1. DNA fragments can easily be discerned, because their extensions fall below the values pertaining to the intact molecules. For the cutoff, we have used the mean value minus 2 times the standard deviation. Resolution broadening can be neglected, because the optical resolution is 1 order of magnitude smaller than the variance. The mean relative extensions $R_{\|}/L$, i.e., the mean extensions divided by the contour length of the molecule, are set out in Figures 2 and 3.

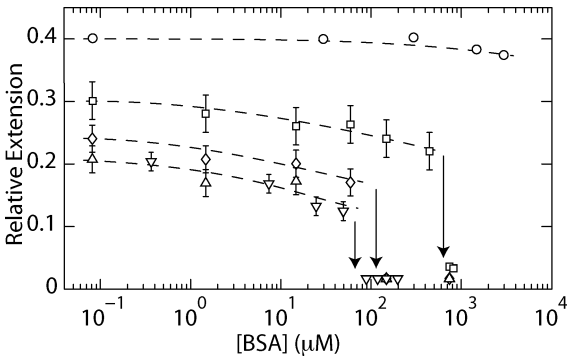

Figure 2. Relative extension $R_{\|}/L$ of T4-DNA in 10 mM Tris/HCl versus the concentration of BSA in 100 × 60 (○), 100 × 250 (□), 200 × 250 (◇), 300 × 200 (▽), and 300 × 250 (Δ) nm^2 channels. The dashed curves are drawn as an aid to the eye.

We first discuss the effect of BSA on the extension of YOYO-1-labeled T4-DNA in 10 mM Tris/HCl (2.9 mM TrisCl, 7.1 mM Tris, pH 8.5) and confined in channels of various cross-sectional diameters (Figure 2). In the channel with a cross-section of 60 × 100 nm^2, the extension is about 0.4 times the contour length. In the wider channels, the relative

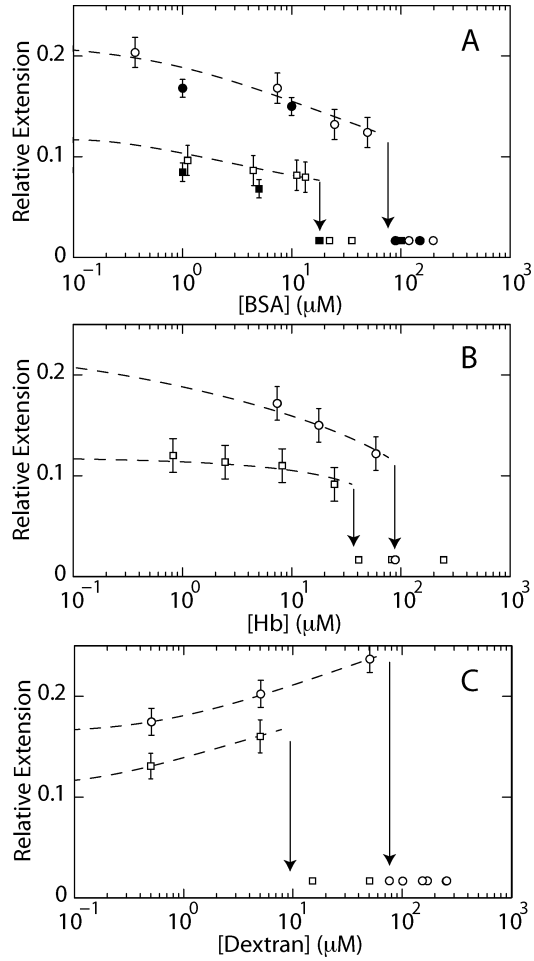

Figure 3. (A) Relative extension $R_{\|}/L$ of T4-DNA (open symbols, YOYO-1 stained) and λ-DNA (closed symbols, Alexa stained) versus the concentration of BSA in 200 × 300 nm^2 channels. (B) $R_{\|}/L$ of T4-DNA versus the concentration of Hb in 200 × 300 nm^2 channels. (C) $R_{\|}/L$ of T4-DNA versus the concentration of dextran (M_w = 50 kDa) in 300 × 300 nm^2 (○) and 200 × 300 nm^2 (□) channels. For all panels, the buffers are 10 mM Tris/HCl (°) or 10 mM Tris/HCl with 25 mM NaCl (□). The dashed curves extrapolate to the protein/dextran-free values at the y-axis, and the arrows demarcate the condensation thresholds.

extensions are in the range of 0.1−0.3. These moderate values of the relative extensions show that the DNA molecules are coiled. With increasing concentration of BSA, the molecules contract in the longitudinal direction of the channel, as shown by a decrease in extension. For overthreshold concentrations of BSA, the DNA molecules condense into a compact form. This condensation is facilitated by the confinement inside the nanospace, because we did not observe condensation in the feeding microchannels and/or the reservoirs of the chip. The critical concentration for condensation shifts to higher values with decreasing channel cross-sectional diameter. In the narrow 60 × 100 nm^2 channel, the molecules remain extended irrespective of the concentration of BSA.

For wider channels, we have investigated the effects of another like-charged protein Hb as well as the neutral crowding agent dextran (Figure 3). The 6.9 nm radius of gyration of the dextran nanoparticles is comparable to the molecular dimensions of the proteins. As in the case of BSA, the addition of Hb initially results in contraction of the DNA molecule. The situation with dextran is somewhat different. Here, the

dx.doi.org/10.1021/jp2124907 | J. Phys. Chem. B 2012, 116, 3031−3036

DNA molecules take a more extended conformation. Irrespective of the agent, the DNA molecules eventually condense into a compact form. The condensation thresholds for BSA, Hb, and dextran are similar. With an increase in ionic strength of the supporting medium by the addition of 25 mM NaCl, the molecules become less extended, and the critical concentrations for condensation shift to lower values.

For most experiments, we have used YOYO-1-labeled T4-DNA with a ratio of one dye molecule per 23 basepairs. We have verified that there is no change in the measured extensions and condensation thresholds if the bis-intercalation ratio is reduced to one dye per 100 basepairs. YOYO-1 carries four positive charges. In order to check whether there are no complications associated with the multivalent and cationic nature of the dye, we have also done experiments with Alexa Fluor 546 labeled λ-DNA. Alexa Fluor 546 is negatively charged through sulfonation, hydrophilic, and covalently linked to uracil bases of the double stranded DNA molecule. As shown in Figure 3, the relative extensions and condensation thresholds obtained with Alexa-labeled λ-DNA molecules are similar to those obtained with YOYO-1-labeled T4-DNA. These similarities as well as the identical results obtained with different YOYO-1 intercalation ratios show that the condensation phenomenon is not related to the dye.

In addition to the nanofluidic experiments, we have investigated how the size of the DNA molecule in the bulk phase changes with the addition of protein. Fluorescence microscopy experiments were done with T4-DNA in 10 mM Tris/HCl and 10 mM Tris/HCl with 100, 200, and 300 mM of added NaCl. We have measured the diameter of the molecules by taking an isotropic average of the fluorescence intensity, despite the fact that the molecules are slightly anisotropic. The distribution in size was observed to be close to Gaussian. The mean diameters, examples of the distribution, and characteristic images are shown in Figure 4. A significant reduction in coil size is observed at high ionic strength and concentrations of BSA on the order of 1 mM. In the case of Hb, we have not observed a significant reduction in coil size due to the limited solubility of Hb (Hb is insoluble for concentrations exceeding 0.1 mM). We have checked that, with a concentration of NaCl less than 100 mM, the diameter of the DNA coil is hardly affected by the protein. For intermediate ionic strengths and concentrations of protein, full and partially compacted molecules were observed to be in coexistence. These findings are in quantitative agreement with those reported by Yoshikawa et al.[16]

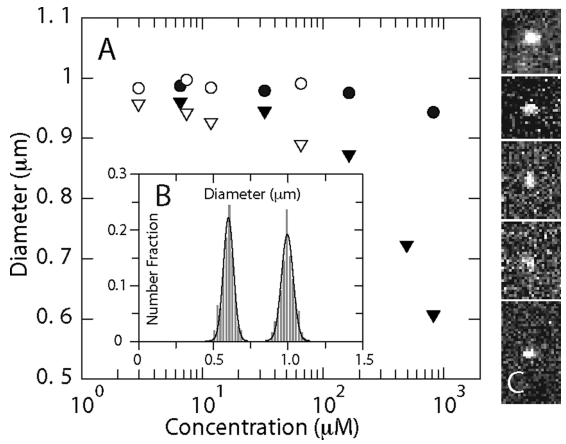

Figure 4. (A) Mean diameter of T4-DNA molecules in the bulk phase versus the concentration of BSA (closed symbols) and Hb (open symbols). The buffers are 10 mM Tris/HCl (○) and 10 mM Tris/HCl with 300 mM NaCl (▽). (B) Distribution in diameter of T4-DNA molecules in 10 mM Tris/HCl (right) and 10 mM Tris/HCl with 300 mM NaCl (left) buffer and 825 μM of BSA. (C) Fluorescence microscopy images of T4-DNA in 10 mM Tris/HCl with 300 mM NaCl and BSA concentrations of 6.6, 33, 165, 495, and 825 μM from top to bottom.

In summary, we arrive at the following features of the behavior of DNA confined in a nanochannel and crowded by like-charged protein. For subthreshold concentrations of protein, the molecules are contracted in the longitudinal direction with respect to the protein-free state. In the wider channels, DNA condenses into a compact form for over-threshold concentrations of protein. The critical concentration for condensation shifts to higher values with decreasing cross-sectional diameter. In a narrow channel with a cross-section of 60 × 100 nm^2, the extension is almost constant, and no condensation is observed. Nanoconfinement facilitates condensation by like-charged protein at a low ionic strength of a few millimolars. In the bulk phase, it is necessary to increase the salt concentration to around 100 mM in order to get a significant fraction of condensed DNA. The critical concentrations of protein for condensation are similar to those obtained for dextran and are in the range of tens to hundreds of micromolars, depending on the cross-sectional diameter of the channel and the ionic strength of the supporting buffer.

IV. DISCUSSION

At the present pH of 8.5, BSA and Hb are negatively charged. Furthermore, they are not known to complex on DNA or to have any specific interaction with DNA. Accordingly, the proteins can easily penetrate the interior of the DNA coil. The protein concentration in the interior of the coil is, however, reduced with respect to the value in the surrounding buffer due to a combination of electrostatic repulsion and hard-core volume interaction. For subthreshold concentrations of protein, the concomitant osmotic pressure gradient results in a contraction of the coil in the longitudinal direction of the channel. In the case of dextran, elongation rather than contraction is observed. This has been discussed before, and is thought to originate from depletion of DNA segments and volume occupancy of neutral nanoparticles in the interfacial region next to the channel wall.[14,15]

The condensation of DNA for overthreshold densities of a crowding agent is well-known.[3] Here, we report condensation inside nanochannels by like-charged protein in 10 mM Tris/HCl buffer with an ionic strength of around 3 mM. This ionic strength is markedly lower than the one employed in polymer and salt-induced (psi) condensation of DNA in the bulk phase.[2] For psi condensation, it is necessary to increase the ionic strength to a value exceeding 100 mM. Condensation of DNA in the bulk phase by like-charged protein is no different in this respect. Furthermore, the critical concentrations for condensation are in the range of tens to hundreds of micromolars depending on the cross-sectional diameter of the channel and ionic strength, but irrespective of the condensing agent. These values are at least an order of magnitude lower than the ones pertaining to condensation in the bulk phase. For instance, the critical concentration for inducing full compaction of DNA by BSA is around 2.3 mM.[16] On the other hand, preliminary experiments on the nanofluidic compaction of DNA by the

dx.doi.org/10.1021/jp2124907 | J. Phys. Chem. B 2012, 116, 3031−3036

cationic nucleoid-associated protein H-NS show a critical concentration of around 1 μM.

Condensation induced by crowders such as dextran or like-charged protein is due to depletion-induced attraction between DNA segments. A cylindrical volume in which the crowder cannot penetrate surrounds each segment. In the case of a like-charged crowder, the diameter of this volume is approximately equal to the sum of the diameter of the DNA duplex, the radius of gyration of the crowder, and 2 times the Debye screening length: $D_{DNA} + R_g + 2\kappa^{-1}$ with $D_{DNA} = 2$ nm.[26] For two parallel cylinders with their center lines of mass separated by a distance r with $D_{DNA} < r < D_{DNA} + R_g + 2\kappa^{-1}$, there is an attractive force due to the exclusion of the crowders from the overlap region. On the basis of an Asakura−Oosawa type of treatment, the interaction energy per unit length is given by the cross-sectional area of the overlap region times the osmotic pressure exerted by the crowders and takes the approximate form

$$\frac{U(r)}{kT} = -\frac{\pi}{4}(D_{DNA} + R_g + 2\kappa^{-1})^2 \times \left[1 - \frac{r}{D_{DNA} + R_g + 2\kappa^{-1}}\right]\rho \quad (1)$$

with ρ being the density of crowders inside the coil.[26,28,27] This expression is strictly valid close to the protein θ point, i.e., for moderately charged proteins with relatively poor solubility. For proteins of higher charge, higher order cross interactions (virials) between DNA and multiple proteins need to be taken into account. As shown by Monte Carlo simulation, this results in a significant increase in protein-induced depletion attraction through an increase in free energy of inserting DNA into the protein solution.[26] There are, however, no qualitative changes in the distance and orientation dependence of the depletion interaction. The attractive depletion interaction is set off against the electrostatic repulsion, leading to a net potential depending on the relative strengths of the electrostatic and depletion interactions. Condensation occurs when the absolute value of the depletion interaction energy exceeds a certain critical value.

It should be noted that an effective depletion interaction requires the juxtaposition of two almost parallel cylindrical segments. Once the segments are skewed, the overlap region is significantly reduced, and the attractive interaction disappears. A plausible mechanism for the nanochannel-facilitated compaction is the increase in contact pairs of (almost) parallel-aligned and juxtaposed segments due to orientation order imposed by the channel walls. The critical concentration for condensation hence depends on two factors: the orientation order and the probability of a contact. With decreasing cross-sectional diameter, the orientation order increases. Concurrently, the contact probability decreases, simply because the correlation length of the volume interaction is on the order of the diameter of the channel. In the blob model of Daoud and de Gennes, the contact probability is proportional to the number of segments per blob, i.e., $\propto D^{5/3}$ with cross-sectional diameter D.[29] The increase in critical concentration with decreasing channel diameter can hence be explained by a decrease in contact probability despite the increase in orientation order. Once the molecule is fully aligned, no juxtaposed contact pairs can be formed, and condensation is suppressed.

V. CONCLUSIONS

Our experiments show that DNA can be compacted by like-charged, nonbinding protein at submillimolar concentrations and low ionic strength. For this purpose, it is necessary to confine the molecule in a quasi one-dimensional nanospace. Geometry is important as shown by the strong dependence of the critical concentration of protein for condensation on the cross-sectional diameter of the channel. Furthemore, in two-dimensional nanoslit confinement, there is no abrupt, but rather a gradual transition of crowded DNA into a compact form.[15] The similarity in condensation thresholds for protein and dextran indicates a depletion mechanism. In nanochannel confinement, the depletion interaction is enhanced due to orientation order imposed by the channel walls. The enhanced depletion interaction results in fairly low critical concentrations of protein for condensation. The depletion interaction decreases with decreasing channel diameter due to progressive screening of volume interaction. However, a moderate confinement is sufficient for a significant impact on the compaction of DNA.

AUTHOR INFORMATION

Corresponding Author

*Electronic mail: johanmaarel@gmail.com.

Notes

The authors declare no competing financial interest.

ACKNOWLEDGMENTS

We acknowledge financial support from the MOE Academic Research Fund MOE2009-T2-2-005 and ASTAR (Singapore) R-144-000-261-305.

REFERENCES

(1) Zimmerman, S. B.; Minton, A. P. *Annu. Rev. Biophys. Biomol. Struct.* **1993**, *22*, 27−65.
(2) Lerman, L. S. *Proc. Natl. Acad. Sci. U.S.A.* **1971**, *68*, 1886−1890.
(3) Bloomfield, V. A. *Curr. Opin. Struct. Biol.* **1996**, *6*, 334−341.
(4) Kojima, M.; Kubo, K.; Yoshikawa, K. *J. Chem. Phys.* **2006**, *124*, 024902.
(5) Walter, H.; Brooks, D. E. *FEBS Lett.* **1995**, *361*, 135−139.
(6) Zimmerman, S. B.; Murphy, L. D. *FEBS Lett.* **1996**, *390*, 245−248.
(7) Murphy, L. D.; Zimmerman, S. B. *Biophys. Chem.* **1995**, *57*, 71−92.
(8) Allen, M. J.; Bradbury, E. M.; Balhorn, R. *Nucleic Acids Res.* **1997**, *25*, 2221−2226.
(9) Zhang, C.; van der Maarel, J. R. C. *J. Phys. Chem. B* **2008**, *112*, 3552−3557.
(10) Reisner, W.; Morton, K. J.; Riehn, R.; Wang, Y. M.; Yu, Z.; Rosen, M.; Sturm, J. C.; Chou, S. Y.; Frey, E.; Austin, R. H. *Phys. Rev. Lett.* **2005**, *94*, 196101.
(11) Persson, F.; Utko, P.; Reisner, W.; Larsen, N. B.; Kristensen, A. *Nano Lett.* **2009**, *9*, 1382−1385.
(12) Reisner, W.; Beech, J. P.; Larsen, N. B.; Flybjerg, H.; Kristensen, A.; Tegenfeldt, J. O. *Phys. Rev. Lett.* **2007**, *99*, 058302.
(13) Zhang, C.; Zhang, F.; van Kan, J. A.; van der Maarel, J. R. C. *J. Chem. Phys.* **2008**, *128*, 225109.
(14) Zhang, C.; Shao, P. G.; van Kan, J. A.; van der Maarel, J. R. C. *Proc. Natl. Acad. Sci. U.S.A.* **2009**, *106*, 16651−16656.
(15) Jones, J. J.; van der Maarel, J. R. C.; Doyle, P. S. *Nano Lett.* **2011**, *11*, 5047−5053.
(16) Yoshikawa, K.; Hirota, S.; Makita, N.; Yoshikawa, Y. *J. Phys. Chem. Lett.* **2010**, *1*, 1763−1766.
(17) Bohme, U.; Scheler, U. *Chem. Phys. Lett.* **2007**, *435*, 342−345.
(18) Lin, S. H.; Hung, C. L.; Juang, R. S. *Desalination* **2008**, *234*, 116−125.
(19) van Kan, J. A.; Bettiol, A. A.; Watt, F. *Appl. Phys. Lett.* **2003**, *83*, 1629−1631.
(20) van Kan, J. A.; Bettiol, A. A.; Watt, F. *Nano Lett.* **2006**, *6*, 579−582.

(21) Shao, P. G.; van Kan, J. A.; Ansari, K.; Bettiol, A. A.; Watt, F. *Nucl. Instrum. Methods Phys. Res., Sect. B* **2007**, *260*, 479−482.
(22) Johansen, F.; Jacobsen, J. P. *J. Biomol. Struct. Dyn.* **1998**, *16*, 205−222.
(23) Bakajin, O. B.; Duke, T. A. J.; Chou, C. F.; Chan, S. S.; Austin, R. H.; Cox, E. C. *Phys. Rev. Lett.* **1998**, *80*, 2737−1740.
(24) Das, S. K.; Austin, M. D.; Akana, M. C.; Deshpande, P.; Cao, H.; Xiao, M. *Nucleic Acids Res.* **2010**, *38*, e177.
(25) Tegenfeldt, J. O.; Prinz, C.; Cao, H.; Chou, S.; Reisner, W. W.; Riehn, R.; Wang, Y. M.; Cox, E. C.; Sturm, J. C.; Silberzan, P.; Austin, R. H. *Proc. Natl. Acad. Sci. U.S.A.* **2004**, *101*, 10979−10983.
(26) de Vries, R. *J. Chem. Phys.* **2008**, *125*, 014905.
(27) Asakura, S.; Oosawa, F. *J. Chem. Phys.* **1955**, *22*, 1255−1256.
(28) van der Maarel, J. R. C. *Introduction to Biopolymer Physics*; World Scientific: Singapore, 2008.
(29) Daoud, M.; de Gennes, P. G. *J. Phys. (Paris)* **1977**, *38*, 85−93.